J. Neural Eng. **6** (2009) 055008 (13pp) doi:10.1088/1741-2560/6/5/055008

Evaluation of probabilistic methods to predict muscle activity: implications for neuroprosthetics

Lise A Johnson[1] **and Andrew J Fuglevand**[1,2,3]

[1] Graduate Program in Biomedical Engineering, University of Arizona, Tucson, AZ, 85721-0093, USA
[2] Departments of Physiology and Neurobiology, University of Arizona, Tucson, AZ, 85721-0093, USA

E-mail: fuglevan@u.arizona.edu

Received 27 February 2009
Accepted for publication 16 July 2009
Published 1 September 2009
Online at stacks.iop.org/JNE/6/055008

Abstract

Functional electrical stimulation (FES) involves artificial activation of muscles with surface or implanted electrodes to restore motor function in paralyzed individuals. Currently, FES-based prostheses produce only a limited range of movements due to the difficulty associated with identifying patterns of muscle activity needed to evoke more complex behaviour. Here we test three probability-based models (Bayesian density estimation, polynomial curve fitting and dynamic neural network) that use the trajectory of the hand to predict the electromyographic (EMG) activities of 12 arm muscles during complex two- and three-dimensional movements. Across most conditions, the neural network model yielded the best predictions of muscle activity. For three-dimensional movements, the predicted patterns of muscle activity using the neural network accounted for 40% of the variance in the actual EMG signals and were associated with an average root-mean-squared error of 6%. These results suggest that such probabilistic models could be used effectively to predict patterns of muscle stimulation needed to produce complex movements with an FES-based neuroprosthetic.

(Some figures in this article are in colour only in the electronic version)

1. Introduction

Functional electrical stimulation (FES) involves the controlled stimulation of one or more skeletal muscles to produce movements in otherwise paralyzed limbs. Many of the substantial difficulties associated with chronic deployment of FES systems have been overcome (Ko *et al* 1977, Keith *et al* 1988, Handa *et al* 1989, Hoshimiya *et al* 1989, Kilgore *et al* 1989, Peckham *et al* 2002) and a growing number of patients are using FES systems to regain some of the function of their upper limbs (Triolo *et al* 1996, Smith *et al* 1987, Peckham *et al* 2001). However, only a few pre-programmed movements are permitted by these systems. This is primarily because of the difficulty associated with identifying the complex patterns of muscle activity needed to produce even relatively simple movements. Most natural movements require coordination of multiple muscles across multiple joints (Schieber 1995, Valero-Cuevas 2000) and such complex systems do not readily lend themselves to deterministic solutions.

An alternative probability-based approach has been used previously by Seifert and Fuglevand (2002) to predict patterns of muscle stimulation needed to produce simple finger movements, and by Anderson and Fuglevand (2008) to predict the activity in muscles associated with complex two-dimensional movements of the arm. The reasonable level of prediction accuracy achieved by these models suggests that probabilistic approaches may provide a flexible means to control FES systems. The probabilistic models used in these previous studies, however, were relatively unsophisticated, and it is reasonable to assume that more refined models might generate better results.

In the present study, we evaluated the ability of three different types of probabilistic models, an unsupervised Bayesian density estimation, a polynomial curve fitting algorithm and a dynamic neural network, to predict the

[3] Author to whom any correspondence should be addressed.

simultaneous activity of multiple muscles in the upper limb during sagittal-plane arm movements. The data used for testing the different algorithms were those acquired previously by Anderson and Fuglevand (2008). For each probabilistic method tested, the inputs to the models were the kinematics of the hand. The analyses indicated that the neural network approach yielded slightly better predictions than the other two methods. We then tested the ability of the neural network model to predict muscle activity associated with three-dimensional movements. The high correspondence between the muscle activity predicted by the neural network model and the recorded muscle activity during three-dimensional movements confirms that this approach may be an effective tool for identifying the complex patterns of muscle activity needed to control a wide range of movements using FES.

2. Methods

2.1. Experimental setup

The data set that served as the 'test-bed' to evaluate different probabilistic methods was that collected and published by Anderson and Fuglevand (2008) where a detailed description of the methods can be found. Here we give only a brief overview of the experimental procedures. Five male subjects participated in the study, each of whom gave informed consent to participate in the study, which was approved by the institutional human subjects committee. As described in more detail below, electromyographic (EMG) and kinematic data from the upper limb were recorded from each subject while they made a variety of sagittal plane movements (figure 1). Subjects sat upright in an armless, low-backed chair. Recording electrodes were placed in bipolar configurations on the surface of the skin over 12 target muscles controlling movements of the upper limb (latissimus dorsi, pectoralis major, serratus anterior, teres major, anterior deltoid, posterior deltoid, triceps brachii, biceps brachii, brachialis, brachioradialis, extensor carpi radialis and flexor carpi radialis). Glow-in-the-dark markers were affixed to the hand (metacarpalphalangeal joint on the ulnar aspect of the hand) and to the shoulder so that their positions could be tracked by video recording.

EMG signals from the 12 muscles were differentially amplified by a factor of 1000, band-pass filtered between 100 and 1000 Hz, and sampled at 2000 Hz. The lower frequency limit of the filter was chosen to minimize movement artefacts (Anderson and Fuglevand 2008).

The positions of the hand and shoulder markers were sampled from video recordings at 30 frames per second. The camera was set up approximately 4 m from the subject and oriented so that the camera axis was aligned perpendicular to the sagittal plane of the subject. A flashing LED generated by the data acquisition system was also recorded by the camera and served as a datum for synchronizing the EMG signals with the kinematic data.

2.2. Experimental procedures

Recording sessions lasted for approximately 18 min. Subjects were asked to perform natural, comfortable, random movements in the sagittal plane while keeping the hand pronated in order to keep the hand marker facing the camera (figure 1). Subjects were asked to move through as many points of the space as possible and to use different speeds. Subjects were encouraged to take short breaks during which time the arm hung pendant at the side. No subjects reported muscle fatigue.

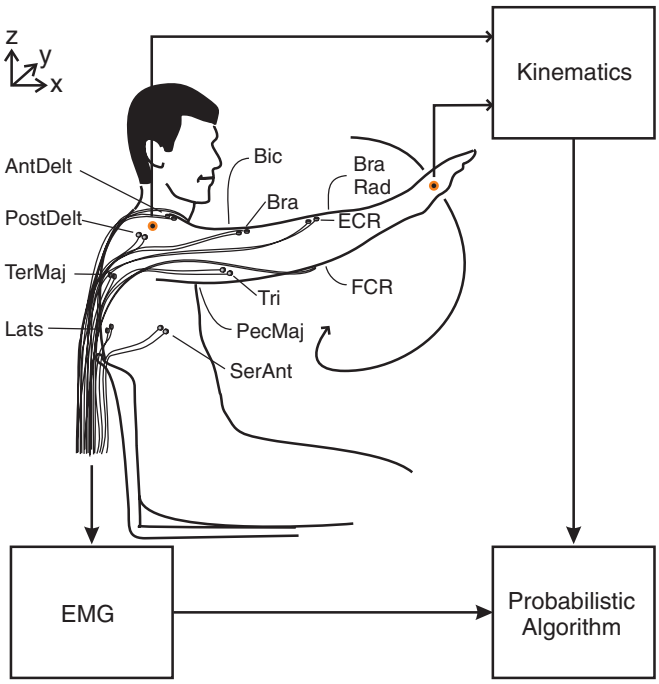

Figure 1. Experimental setup. Surface EMG signals from 12 arm muscles and kinematic data from markers placed on the hand and shoulder were recorded during sagittal-plane random movements. These data served as inputs to one of three probabilistic algorithms that characterized the relation between EMG and kinematics. Once a probabilistic algorithm was trained, a new set of kinematic data served as inputs to the algorithm in order to predict the associated patterns of EMG activity across the 12 muscles (Lats: latissimus dorsi, Pec Maj: pectoralis major, Ter Maj: teres major, Ser Ant: serratus anterior, Ant Delt: anterior deltoid, Post Delt: posterior deltoid, Tri: triceps brachii, Bic: biceps brachii, Bra: brachialis, Bra Rad: brachioradialis, ECR: extensor carpi radialis, FCR: flexor carpi radialis) (adapted from Anderson and Fuglevand (2008)).

2.3. EMG processing

All off-line processing was performed in Matlab (*Mathworks*, Natick, MA). In accordance with conventional processing methods (Winter 2005), EMG signals were full-wave rectified and low-pass filtered at 6 Hz (sixth order, Butterworth, zero phase). EMG signals were subsequently downsampled to match the sampling frequency of the kinematic data and normalized to the maximum amplitude detected in the signal. A fixed delay of 60 ms was added to the EMG signals to compensate for the time lag between EMG activity and kinematics (Manal and Rose 2007).

2.4. Kinematic processing

The sagittal-plane locations of the hand and shoulder markers were identified in each frame of the video recordings using

automated digitizing software. These data were then low-pass filtered at 6 Hz (sixth order, Butterworth, zero phase). Position data of the hand were expressed in terms of a shoulder-based coordinate system in which the shoulder marker represented the origin. The x (horizontal) and z (vertical) components of the hand marker were scaled by the maximal displacement of the hand detected over the entire recording session. Single and double differentiation of the x- and z-components of the processed hand-position data were performed to obtain horizontal and vertical velocities and accelerations of the hand.

2.5. Probabilistic models

Three model architectures were used to represent different classes of probabilistic regression: Bayesian density estimation, polynomial curve fitting and a neural network. These categories were selected because they are commonly used for science and engineering applications. Furthermore, Bayesian density estimation has been used previously by Seifert and Fuglevand (2002) and Anderson and Fuglevand (2008) to predict patterns of muscle activity. Polynomial curve fitting was included because it is a simple method to establish a predictive relationship. Finally, we chose to use a neural network partly because neural networks have been used to fit the forward problem, namely to predict kinematics from EMG signals (Au and Kirsch 2000, Cheron *et al* 1996, Koike and Kawato 1995), and partly because neural networks have been extensively used to solve a variety of nonlinear problems.

All of the models that we tested relied on some dimensionality reduction as a way to mitigate the problem of inter-dependent input variables while at the same time reducing the computational burden of the algorithms. To this end, we applied a principal components analysis (PCA) to the kinematic input vector. PCA is a linear transformation that uses the covariance of the variables to find the optimal linear reduction of the data from m dimensions down to n dimensions. While the principal components are uncorrelated with each other, they are only linearly independent if all of the variables have a Gaussian distribution. If the data sources are normally distributed, then they are completely described by their second-order statistics, and PCA provides the optimal separation of the data (Hyvarinen 1999). Dimensionality is reduced by choosing the first n components.

We constructed a six-dimensional vector composed of the horizontal and vertical positions (x, z), velocities (v_x, v_z) and accelerations (a_x, a_z) of the hand to represent the kinematic state of the limb. Depending on the data set, the first principal component accounted for 40–70% of the variance in the full kinematic vector. Inclusion of additional principal components (PC) dramatically increased the computational load, particularly for the Bayesian-based model, without markedly increasing prediction accuracy. Therefore, the first principal component was used as the input for all of the algorithms. In some test cases (see section 3), we quantified the effect of including higher-order principal components on the ability of the models to predict EMG.

2.6. Unsupervised Bayesian density estimation

For this model, the joint probability distribution between the EMG signal and kinematic state for each muscle was determined from the training data (the characteristics of the training data sets are described in detail below). This distribution was then conditioned, according to Bayes' theorem, on a prior distribution, which took into account the kinematic state at previous time steps. The prior was constructed by low-pass filtering the kinematic data with a 15-sample (0.5 s) linear-ramped window. In this way, a linearly decreasing amount of information from the past was represented in the kinematic state at any given time point. The inclusion of data from multiple time points and the dimensionality reduction of the input vector by PCA represent major differences between our Bayesian model and that used previously by Anderson and Fuglevand (2008). A joint probability density distribution between the time-shifted version of the kinematics and the EMG activity was then determined. Thus, the total probability distribution was

$$P(\mathrm{EMG}_j|\mathrm{Kin}) = \frac{P(\mathrm{Kin}|\mathrm{EMG}_j) \cdot P(\mathrm{EMG}_j|\mathrm{Kin_{TS}})}{P(\mathrm{Kin})}, \quad (1)$$

where EMG_j is the EMG activity of the jth muscle at a particular instant in time, Kin is the first principal component of the kinematic state, and $\mathrm{Kin_{TS}}$ is the time-shifted version of the reduced kinematic state. Predictions of EMG amplitude for new kinematic inputs were made by finding the expected value of $P(\mathrm{EMG}_j|\mathrm{Kin})$ evaluated at each time point.

2.7. Polynomial curve fitting

For this model, dimensionality of the kinematic data vector was again reduced to the first principal component. For each muscle, EMG was plotted as a function of the reduced kinematic parameter, and a third-order polynomial curve was fit to these points using linear least squares. A third-order polynomial was used because it captured the dynamics of the system without over-fitting. Predictions of EMG amplitude for new kinematic inputs were then made by evaluating the polynomial at each time point.

2.8. Dynamic neural network

As for the other two models, the kinematic input vector was reduced to one principal component. The training data (described below) were mapped to zero mean and unit amplitude representations. A feed-forward, time-delayed neural network with four hidden layers was created using the Matlab Neural Networks Toolbox. The first hidden layer had 20 neurons, the second and third layers each had 9 neurons, and the fourth layer had 20 neurons. The network was built with two time delays; the kinematic vectors from the two immediately preceding time points were included as inputs. The network was fully connected so that in every layer all of the neurons received all of the outputs from the previous-layer neurons, or in the case of the input layer, all of the kinematic inputs. Hyperbolic tangent sigmoidal transfer functions were used for each of the hidden neuron layers. At the output

layer, the 20 neurons were fully connected to the 12 muscle outputs with a linear transfer function. The network was initialized with random weights and biases and trained for 100 iterations using gradient descent with momentum weight and bias learning function, the resilient backpropagation training function and a mean-squared error performance function. After the network was trained, new predictions were made by preprocessing the testing data in the same way as the training data and finding the output of the network. Predictions were low-pass filtered with a 10-point moving average filter to remove high-frequency deflections. This final filtering step was not necessary for the other two models as the outputs were already highly smoothed.

The particular architecture of the neural network used here was chosen based on an iterative approach that began with a single layer network with one neuron and then progressively increased the number of neurons to 100. Each network was trained five times and used to predict a novel data set. The average error was found for each network and the approximate number of neurons at which the average error did not appear to continue to improve appreciably (based on visual inspection) was selected. An additional layer was then added to the network, and the same iterative process was performed on the new layer. This was repeated for all four layers of the network and for the delay parameter (which ran between 0 and 10). On this basis, we ended up with a final network with 20 neurons in the first layer, 9 neurons in the second and third layers, 20 neurons in the fourth layer, and two time delays.

2.9. Over-fitting

It is possible that a model may over-fit the specific data set used for training, and thereby may begin to predict noise in the training set rather than tracking the underlying relationship. To determine if the Bayesian or polynomial models were over-fit to the training data, a portion of the training data was reserved as a validation set and not used in the training. After the model was trained, predictions were generated for a series of randomly chosen portions of the training set and the validation set. For both the Bayesian and polynomial models, the prediction errors for the training data and the validation data were not different from one another, suggesting that the models were not over-fit. Likewise for the neural network, a portion of training data was set aside to serve as a validation set. For each iteration of training, the ability of the neural network to predict the validation set was assessed. If the predictions of the validation set stopped improving, then training was halted (called 'early stopping'). The network, however, always reached the maximum number of training epochs before it was terminated by early stopping.

2.10. Data analysis

Kinematic and EMG data were recorded from five able-bodied male volunteers during approximately 18 min of random arm movements in the sagittal plane. Analyses were carried out using two compositional forms of training data. For one form, which we refer to as *within-subject* training, the data used to train the algorithms, and the data used for testing the algorithms, were obtained from the same subjects. This represents a best-case scenario for prediction because subject differences in the relationship between EMG and kinematics do not contaminate predictions. For the other form, referred to as *across-subject* training, data recorded from each subject, in turn, were used to train the algorithms, while data obtained from the other subjects were used to test the predictions of the algorithm. This form of training provides a more realistic evaluation of the probabilistic approaches associated with the development of an FES controller, which by necessity, would need to be trained on able-bodied subjects and deployed in paralyzed individuals.

For within-subject training, multiple training and testing sets were extracted from the ∼18 min (1100 s) time series by designating different sections of the data as testing and training data. Each testing set consisted of 100 s of data; the rest of the data set (excluding the testing data) was used as the corresponding training data (about 1000 s). In the first 'trial', the initial 100 s were used as the test data and the subsequent 1000 s were used as training data; in the second trial, the second 100 s were used as the test data and the first 100 s plus the last 900 s were used as training data; in the third trial, the third 100 s were used as the test data and the first 200 s plus the last 800 s were used as the training data, etc. In this way, 11 non-overlapping trials were extracted from each full data set. For the across-subject training, the full data set collected from one subject was used as the training data, and the 11 non-overlapping 100 s partitions of data from each of the other subjects were used as the test data. In repeated runs, each subject in turn provided the data that served as the training set.

Two performance metrics were used to quantify the quality of the predictions made by each model; the squared correlation coefficients (r^2) and the root-mean-squared (RMS) error. The r^2 value, or the coefficient of determination, indicates the amount of variance in the recorded EMG signal that is explained by the predicted EMG signal. This measure is not sensitive to the absolute amplitudes of the signals, but rather it indicates how closely the activity patterns are matched. This was our primary performance measure. The secondary metric, RMS error, represents the average difference in the amplitudes of the two signals at every time point. RMS error values are expressed in terms of normalized EMG units, namely, as a percentage of the peak EMG detected during the 18 min recording. A highly accurate prediction will have an r^2 value approaching one and an RMS-error value approaching zero. These two performance indicators were calculated for each muscle over each trial, where a trial indicates a 100 s segment of test data. The r^2 and RMS error values were then averaged across the 11 trials for each muscle and subject.

Repeated measures ANOVA was performed on r^2 values and on RMS-error values, using algorithm or muscle as factors. This was done separately for predictions based on within-subject training and for predictions derived from across-subject training. The main goal of this analysis was to determine if certain algorithms were more effective at predicting EMG from kinematics than others. A secondary goal was to ascertain whether EMG signals were better

predicted for some muscle than others. *Post-hoc* analyses using pair-wise multiple comparisons were carried out using the Holm–Sidak method (Holm 1979). Data are reported as means (±SD) and the level chosen for significance in the statistical tests was $p < 0.05$.

Finally, based on these statistical analyses and the mean values of r^2 and RMS error, we identified one algorithm that yielded the best predictions of EMG from kinematics. We then tested the general capacity of that algorithm to make predictions on a new data set that involved three-dimensional arm movements. EMG data from the same 12 muscles monitored for the planar-movement experiments were recorded for 15 min while a male subject made random movements of the hand in the three-dimensional seated workspace. The subject was encouraged to include supination/pronation, flexion/extension and ulnar/radial deviation movements at the wrist during this task. Three-dimensional (x, y, z) position data as well as pitch, roll and yaw orientations of the hand were recorded using small electromagnetic sensors (Liberty System, Polhemus, Colchester, VT, USA) attached to the back of the hand and to the shoulder. EMG and kinematic data were then processed as described earlier. For this three-dimensional data set, the inputs to the model consisted of the positions, velocities and accelerations (x, y, z, v_x, v_y, v_z, a_x, a_y, a_z) as well as the pitch, yaw and roll orientations of the hand. This 15 min data set was broken into multiple trials in the same way as described earlier for the two-dimensional experiments, which yielded a total of seven testing/training sets.

3. Results

3.1. Within-subject training

Examples of within-subject training predictions generated by the three models are shown in figure 2 for three different muscles, triceps brachii (figure 2(A)), pectoralis major (figure 2(B)) and anterior deltoid (figure 2(C)). In each panel, the black traces indicate the actual EMG recorded during a single 100 s trial, and the red traces indicate the predicted signals based on hand kinematics. Within each panel, the actual EMG signal is replicated three times to aid in visual comparison to each of the predicted signals. The probabilistic model used for each prediction is indicated immediately above each trace pair, and the associated coefficient of determination (r^2) between predicted and actual EMG is shown for each case. All three models performed reasonably well in that the predictions matched both the amplitude and the temporal dynamics of the recorded signal. This was especially the case for the triceps brachii (figure 2(A)) and for the anterior deltoid (figure 2(C)). As has been reported previously (Soechting and Flanders 1997, Anderson and Fuglevand 2008), predictions for pectoralis major were not as good as for other shoulder muscles, likely because of the limited activity of this muscle in the performance of unloaded movements. For all three muscles, the neural network performed slightly better than either of the other two algorithms.

Figure 3(A) shows the r^2 values, averaged across the five subjects, for each muscle and for each algorithm based

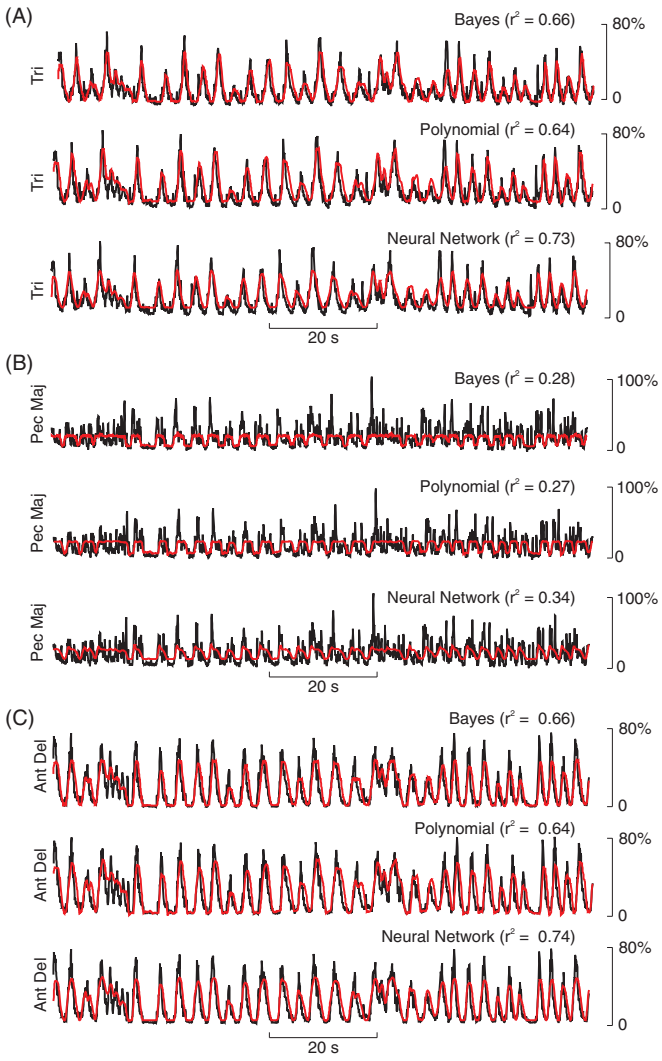

Figure 2. Within-subject training predictions for three muscles. Example predictions made by each of the models (Bayesian density estimation, polynomial curve fitting and dynamic neural network) for triceps brachii (A), pectoralis major (B) and anterior deltoid (C). All three muscles were recorded simultaneously in the same subject; the models were trained by different data recorded from that same subject. The black lines correspond to the actual EMG and the red lines correspond to the predicted EMG. Within each panel, the actual EMG signal is replicated three times to aid in visual comparison to each of the predicted signals. The coefficient of determination (r^2) between predicted and actual EMG is shown for each case. The triceps brachii and the anterior deltoid were better predicted than the pectoralis major. In every muscle, the neural network made better predictions than the other two models. Vertical scale—% peak EMG.

on within-subject training data. For clarity, the standard deviations are not depicted here. Likewise, figure 3(B) shows the averaged RMS errors for each muscle and algorithm. Overall, there was a general tendency for the neural network to predict EMG with slightly higher r^2 values (figure 3(A)) and with modestly lower RMS errors (figure 3(B)). Analysis of variance indicated a significant effect of algorithm ($p < 0.001$) on r^2 values and RMS error for the within-subject predictions of EMG signals. The average r^2 values for the three algorithms were 0.34 ± 0.04, 0.32 ± 0.03 and 0.36 ±

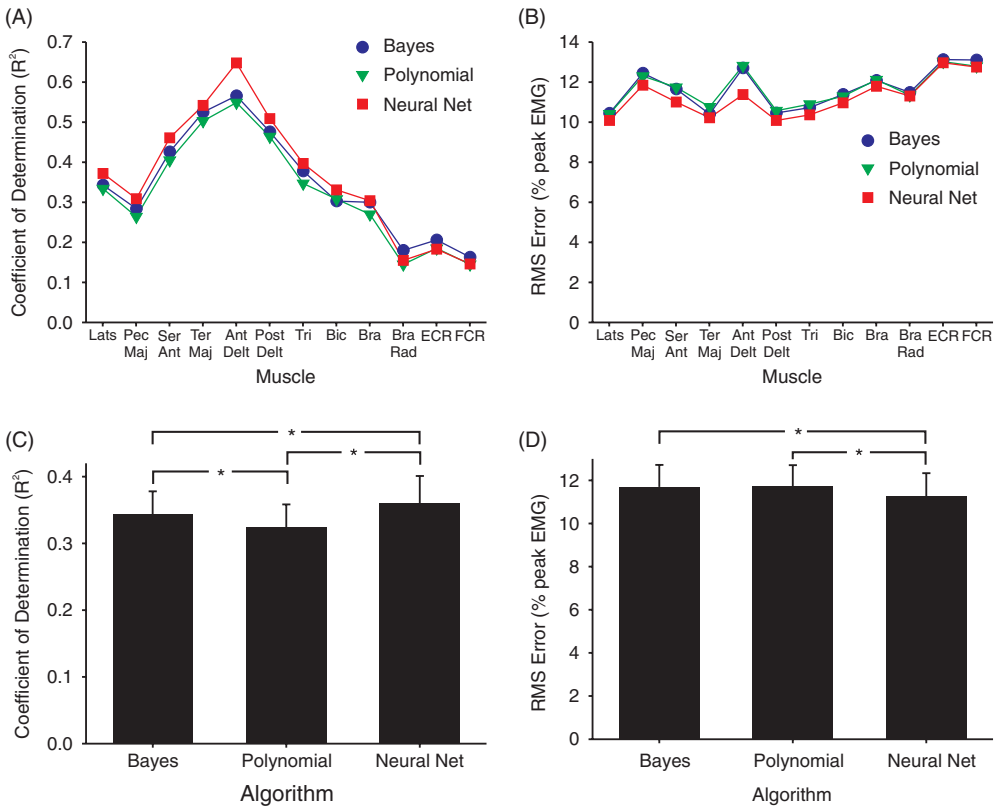

Figure 3. Mean r^2 values (A) and mean RMS errors (B) averaged across the five subjects, for each muscle (abbreviations as used in figure 1) and for each algorithm (Bayesian density estimation: circles, polynomial curve fitting: triangles and dynamic neural network: squares) based on within-subject training data. For clarity, the standard deviations are not depicted. (C) Mean (SD) r^2 values and (D) RMS errors between predicted and actual EMG signals for three prediction models (Bayesian density estimation, polynomial curve fitting, dynamic neural network) based on within-subject training. The neural network yielded significantly larger r^2 values (A) and lower error values (B) than the other two methods (* $p < 0.01$).

0.04 for the Bayesian density estimation, the polynomial curve fit and the neural network, respectively (figure 3(C)). *Post-hoc* analysis indicated that r^2 associated with the neural network was significantly greater ($p < 0.01$) than that associated with either of the other methods, and r^2 for the Bayes method was significantly greater ($p < 0.01$) than that for the polynomial method. Likewise, analysis of variance on RMS error indicated a significant effect of algorithm ($p < 0.001$). The RMS error values were 11.7 ± 1.0, 11.7 ± 1.0 and 11.2 ± 1.1% peak EMG for the Bayes, polynomial and neural network models, respectively (figure 3(D)). *Post-hoc* analysis indicated that RMS error for the neural network model was significantly ($p < 0.01$) less than that of either of the other two models. According to both assessment metrics (i.e. large r^2 and small RMS error), the performance of the neural network model was marginally, though significantly, better than the performance of the other two.

As is evident in figure 3(A), the activities of some muscles were better predicted than others. The order of the muscles presented in this figure is roughly from most proximal to most distal. The muscles that operate directly on the shoulder appeared to be the best predicted (in terms of r^2 values), namely, anterior deltoid, teres major and posterior deltoid, while the most distal muscles were least well predicted. This is probably a function of the extent to which such shoulder muscles were called upon to perform the type of movements associated with the sagittal-plan task (Soechting and Flanders 1997). Analysis of variance indicated a significant effect of muscle on r^2 ($p < 0.001$). *Post-hoc* analysis indicated that the r^2 value for anterior deltoid (Ant Delt) was significantly greater ($p < 0.001$) than that for Bra Rad, ECR and FCR. The only other significant ($p < 0.001$) pair-wise muscle comparisons were between teres major (Ter Maj), and ECR and FCR. There was no significant effect of muscle, however, on RMS error, with all muscles predicted with error of ∼10–13% (figure 3(B)).

3.2. *Across-subject training*

To determine if the solutions generated by the probabilistic models were transferable across subjects, training data acquired from each subject were used to predict EMG signals in the other subjects. Due to an incompatible position reference scheme used with the first subject, only four of the original five subjects' data were included in this analysis. Figure 4 shows examples of the across-subject predictions for each of the three algorithms. The same muscles and test trial are shown in figure 4 as in figure 2 to enable comparisons across the two forms of training data. Not surprisingly, in these examples, the r^2 values tended to be smaller for the across-subject training predictions (figure 4) compared to the within-subject training (figure 2), with the exceptions of anterior

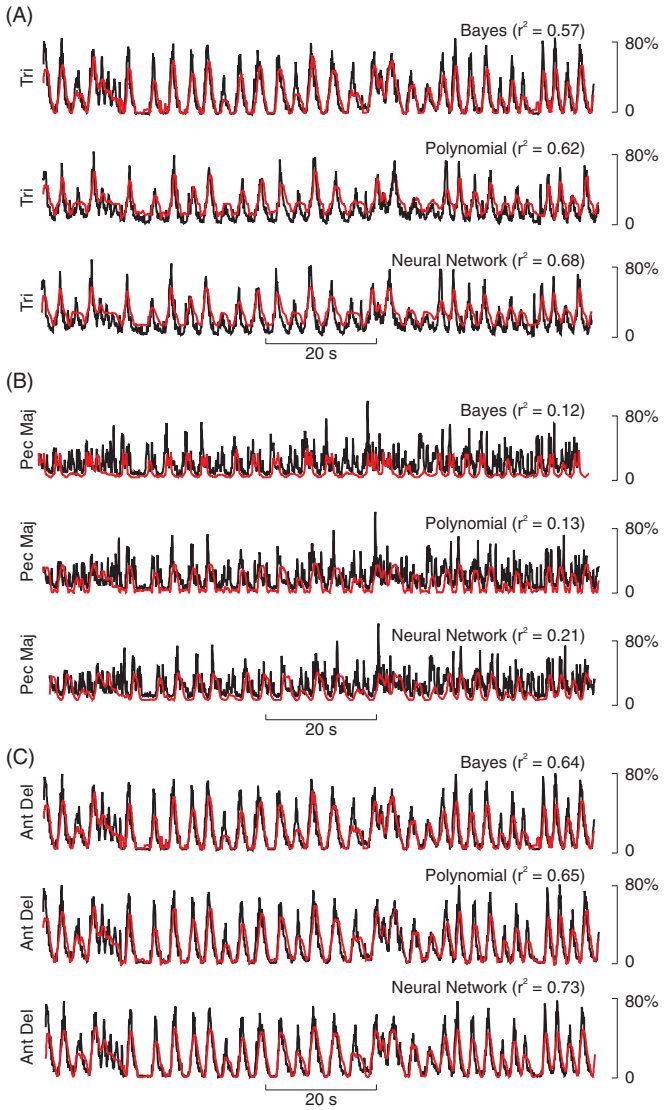

Figure 4. Across-subject training predictions for three muscles. Example predictions made by each of the models (Bayesian density estimation, polynomial curve fitting and dynamic neural network) for triceps brachii (A), pectoralis major (B) and anterior deltoid (C). The format and the example trials are the same as for figure 2. As before, all three muscles were recorded simultaneously in the same subject; however, the predictions shown here were made by models that were trained on data recorded from a different subject. The accuracy of the across-subject training predictions was not as high as for the within-subject training predictions, but the overall pattern of predictability was the same: triceps brachii and anterior deltoid were predicted better than pectoralis major and the neural network tended to make the best predictions for all three muscles.

deltoid, which was predicted with more or less equivalent accuracy for the two sources of training data.

Figures 5(A) and (B) show the r^2 values and RMS errors, averaged across four subjects, for each muscle and for each algorithm based on across-subject training data. Overall, predictions were not as accurate for across-subject training (r^2: 0.24 ± 0.04, 0.26 ± 0.01, 0.28 ± 0.01; RMS error: 14.8 ± 0.7, 14.4 ± 0.4, $14.1 \pm 0.2\%$ peak EMG, for Bayes, polynomial and neural network algorithms, respectively) (figures 5(C) and (D)) as compared to within-subject training. While there was a weak tendency for EMG predictions based on the neural network to exhibit higher r^2 values and lower RMS errors, these differences were not significant ($p = 0.124$ and $p = 0.061$, respectively).

The pattern of prediction accuracy for the different muscles based on across-subject training was generally consistent with that which was observed for the within-subject training predictions. Muscles operating primarily on the shoulder and scapula were better predicted (i.e. higher r^2 values, figure 5(A)) than those acting on the elbow, which in turn, tended to be more accurately predicted than those acting at the wrist.

3.3. Kinematic representation

We applied PCA to the original kinematic input vector as a way to reduce the computational load and to avoid the problem of lack of independence among the kinematic variables. For all of the algorithms tested, we used only the first principal component of the full kinematic vector. Figure 6(A) shows an example of a short time segment of test data depicting the first principal component (red trace) repeatedly overlaid upon each of the corresponding kinematic-variable traces. About half way through this example, the subject paused briefly with the arm pendant at their side before continuing with movements. In this example, there was a high correspondence between the first principal component and the horizontal position of the hand. Indeed, as shown in figure 6(B), the weighting coefficients for the first principal component were largest for the horizontal (x) position and next largest for the vertical (z) position of the hand in all subjects. In addition, there was a remarkable consistency across the five subjects in terms of the pattern of weighting coefficients associated with the first principal component. Overall, these results indicate that for these sagittal plane movements, the horizontal position of the hand was the dominant kinematic feature.

In order to evaluate the effect of including higher-order principal components on the ability of the models to predict EMG, we re-performed the analyses on the within-subject training data using the first two principal components of the kinematic vector rather than just the first. Inclusion of two principal components had no significant effect when using the Bayes algorithm on the average r^2 value (0.29 ± 0.07, $p = 0.18$, paired t test) or RMS error ($12.2 \pm 0.6\%$, $p = 0.26$) compared to that in which only the first principal component was used (see section 3.1). In contrast, prediction accuracy improved significantly ($p < 0.01$, paired t tests), in terms of increased r^2 values and lowered RMS errors, when using two principal components compared to one for the polynomial algorithm ($r^2 = 0.40 \pm 0.04$; RMS error $= 10.8 \pm 1.0\%$) and for the neural network ($r^2 = 0.42 \pm 0.05$; RMS error $= 10.6 \pm 1.2\%$). Therefore, as might be expected, additional information tends to increase the accuracy of the predictions, at least for the polynomial and neural network algorithms. The probable reason that the Bayes algorithm failed to show improvement was that there were insufficient data in the training set to fully characterize the increased dimensionality of the kinematic space.

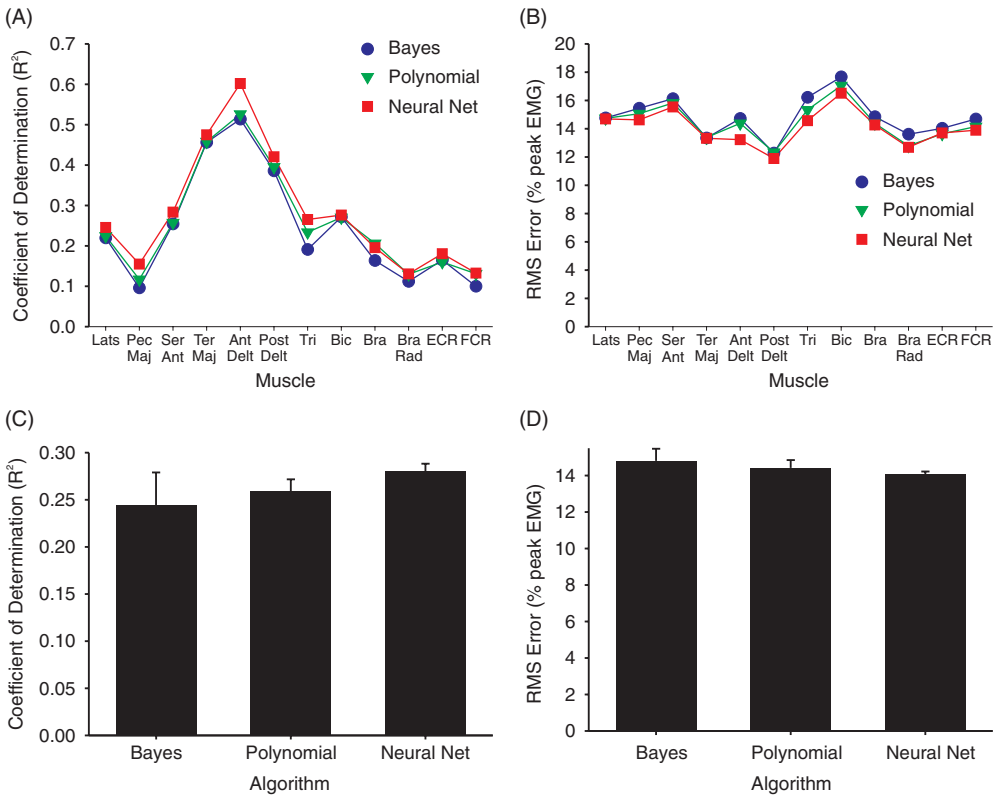

Figure 5. Mean r^2 values (A) and mean RMS errors (B) averaged across four subjects, for each muscle (abbreviations as in figure 1) and for each algorithm (Bayesian density estimation: circles, polynomial curve fitting: triangles and dynamic neural network: squares) based on across-subject training data. For clarity, the standard deviations are not depicted. (C) Mean (SD) r^2 values and (D) RMS errors between predicted and actual EMG signals for three prediction models (Bayesian density estimation, polynomial curve fitting, dynamic neural network) based on across-subject training.

3.4. Model selection

One of the objectives of this study was to choose the most appropriate model for predicting EMG amplitude given the trajectory of the hand. Our results indicate that all three models were effective. However, the neural network model performed significantly better according to both r^2 and RMS error metrics on the within-subject training predictions, and there was a non-significant trend towards better predictions for across-subject training. Furthermore, as indicated above, it may be desirable to increase the dimensionality of the input vector, particularly when attempting to predict more complex movements or movements in three dimensions by including higher-order principal components. The inclusion of additional components is readily accomplished with the neural network but is computationally taxing for the other methods. On the basis of slightly better predictions and practical considerations related to computational efficiency when dealing with higher dimensionality, we chose the neural network algorithm as the best model for this type of prediction task.

3.5. Reaching task

As an extra validation and to provide a reference for comparison to other work, we used the neural network to predict simple reaching movements. Figure 7 shows examples of across-subject predictions of the neural network model for a series of ten repeated reaching movements to one of three targets in the sagittal plane (a high target, a middle-height target and a low target). For each reaching movement, the subject started from a rest position with the arm pendent, and then reached to a self-specified location as if touching a target (though no real target existed) with the arm fully extended, and then returned the hand to the starting position. For the high target (figure 7(A)), subjects reached to a location above the head and in front of the body; for the middle target, subjects reached to a location about shoulder level (figure 7(B)), and for the low-reaching task, subjects reached to a location about knee level (figure 7C). As seen for random movements (figures 2 and 4), predictions were best for the anterior deltoid and triceps, and not as good for pectoralis major (figure 7). Therefore, as was shown previously by Fuglevand and Anderson (2008), predictions of EMG activity for episodic reaching movements are similar to those associated with continuous random movements.

3.6. Three-dimensional test

In order to test whether the neural network algorithm would be as effective for predicting more complex movements, a three-dimensional data set was also recorded and analysed. In this experiment, the subject made a series of unconstrained arm movements, including free wrist movements, in three

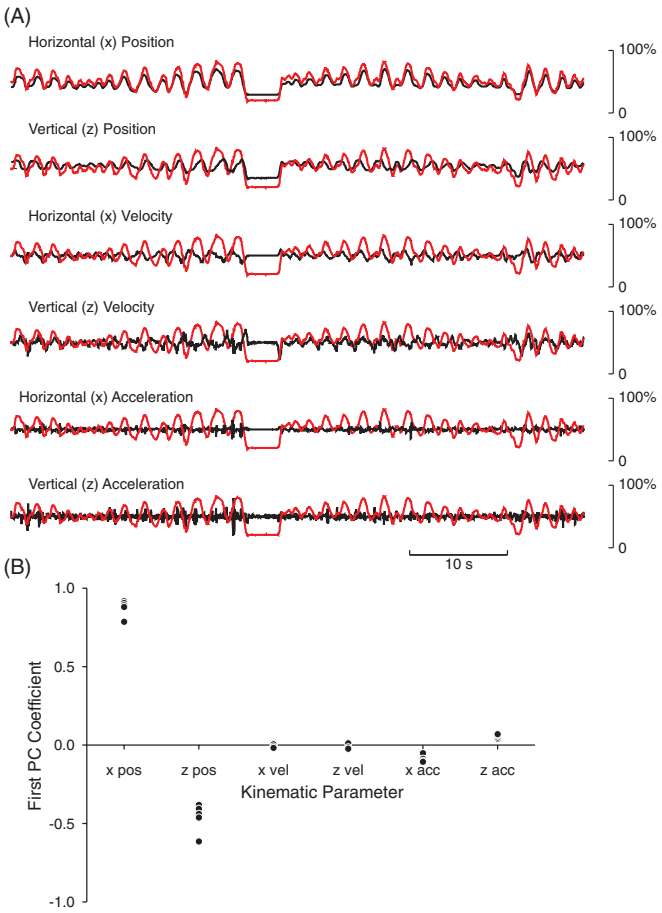

Figure 6. (A) Example time segment depicting the first principal component (red trace) repeatedly overlaid upon each of the corresponding kinematic-variable traces. (B) The weighting coefficients for the first principal component (PC) associated with each of the six kinematic parameters in the original input vector. For each kinematic variable, each dot represents the value of the first PC coefficient for a single subject.

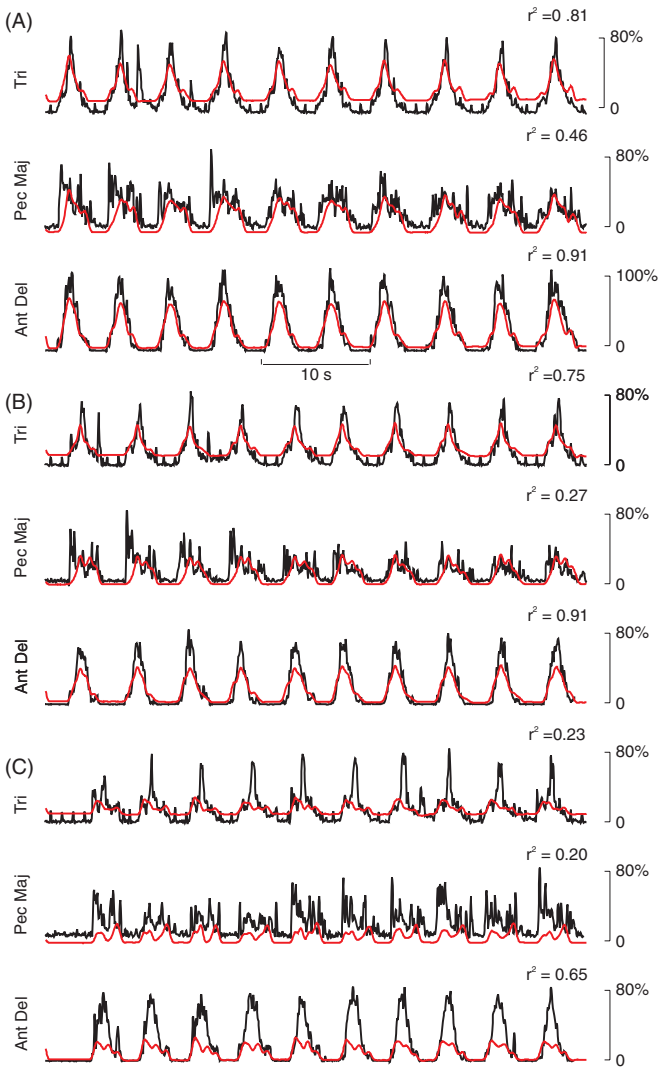

Figure 7. Examples of across-subject predictions of activities of three muscles (triceps brachii, pectoralis major and anterior deltoid) based on the neural network model for a series of ten repeated reaching movements to one of three targets in the sagittal plane: a high target (A), a middle-height target (B) and a low target (C). The black lines correspond to the actual EMG and the red lines correspond to the predicted EMG.

dimensions. Surface EMG signals from the same set of muscles were recorded. At the same time, the pitch, yaw and roll, and the positions (x, y, z), velocities (v_x, v_y, v_z) and accelerations (a_x, a_y, a_z) of the hand relative to the shoulder were measured. To deal with the increased complexity introduced by these additional kinematic parameters, the neural network was slightly modified. Dimensionality was not reduced with PCA, and the number of neurons in the two intermediate layers was increased from 9 to 20 each.

Figure 8 shows a small time segment of some of the kinematic data (x, y and z positions of the hand) and processed EMG signals from the 12 muscles recorded during this task. Example predictions generated by this model are shown in figure 9. In figure 9(A), the same three muscles depicted in previous figures for two-dimensional movements (i.e., figures 2, 4 and 7) are presented for comparison. Predictions of EMG activity for these three muscles during three-dimensional movements were not as good as they were for those associated with two-dimensional movements. On the other hand, some other muscles were predicted better in three-dimensional compared to two-dimensional movements. Examples of three such muscles are shown in figure 9(B).

Figure 10 shows the mean (SD) of the r^2 values for all 12 muscles averaged across the seven test trials in this subject. Overall, muscles that were well predicted in the two-dimensional tests were not necessarily the same muscles that were well predicted in the three-dimensional tests. Most notably, the FCR, a wrist muscle, was the best predicted muscle in the three-dimensional case while it was the least well predicted for two-dimensional movements. This difference can probably be attributed to the additional wrist movements that were allowed in these tests; increasing the proportion of the total movement that the muscle was directly responsible for increased the predictability of the muscle from the movement. When averaged across all muscles, the r^2 value for predictions involving three-dimensional movements

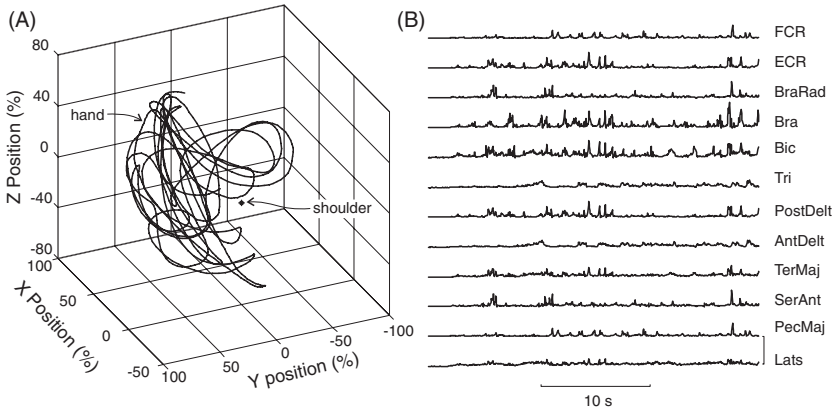

Figure 8. Example segment of training data recorded in one subject during three-dimensional random movements. (A) Hand trajectory (*X*-axis: anterior/posterior, *Y*-axis: medial/lateral, *Z*-axis: superior/inferior relative to shoulder). (B) Rectified, filtered EMG signals from 12 arm muscles. Scale bar for EMG signals is the same for all traces and represents 50% peak EMG (abbreviations as used in figure 1).

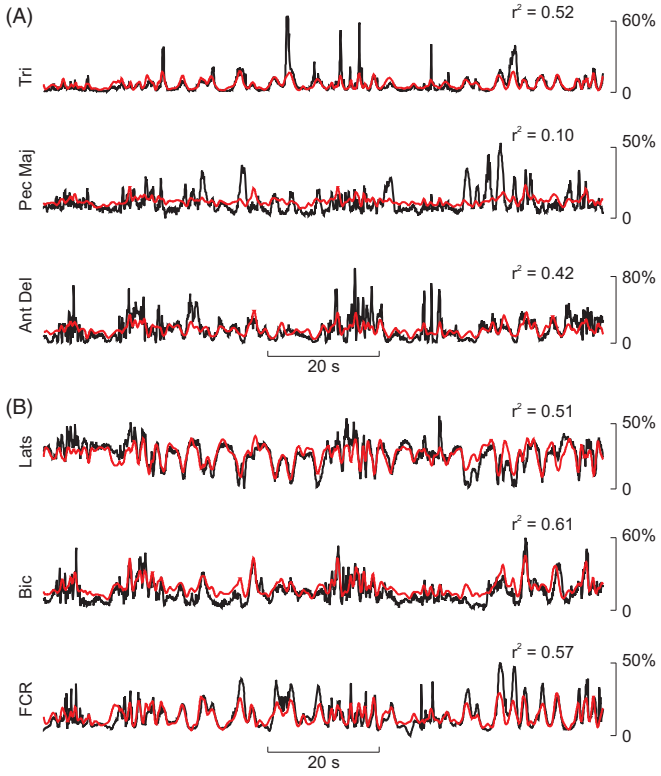

Figure 9. Predictions for three-dimensional movements made by the neural network for (A) triceps brachii (top), pectoralis major (middle) and anterior deltoid (bottom). These muscles are the same as those shown for the two-dimensional examples in figures 2, 4, and 7. The black lines are the recorded signals and the red lines are the predicted signals. (B) Predictions for a different set of muscles: latissimus dorsi (top), biceps (middle) and flexor carpi radialis (bottom), and posterior deltoid (bottom). These three muscles were better predicted in the 3D experiments than they were in the 2D experiments.

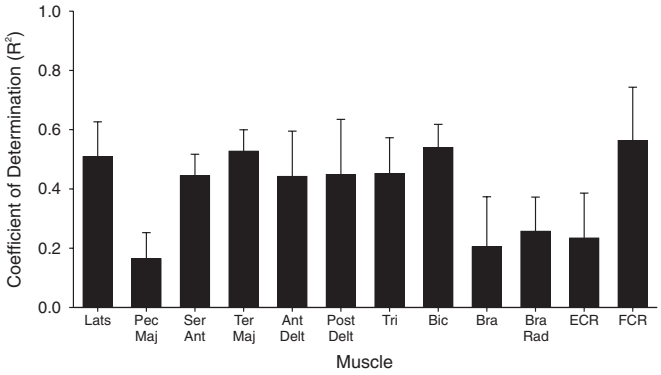

Figure 10. Mean (SD) r^2 values between predicted and recorded EMG signals across different muscles using the neural network applied to three-dimensional movements. The best predicted muscle here (FCR) was the least well predicted for the two-dimensional movements. Abbreviations as in figure 1.

was 0.40 ± 0.18. The overall average RMS error for predictions based three-dimensional movements was 5.9 ± 2.2% of peak EMG. Therefore, the neural network model predicted, with good fidelity, patterns of muscle activity based on hand-trajectory information associated with complex three-dimensional movements.

4. Discussion

Previous studies have shown that probability-based models can effectively predict EMG amplitudes given kinematic parameters representing movements of the hand (Seifert and Fuglevand 2002, Anderson and Fuglevand 2008). In this study, we implemented three different types of probabilistic regression models in order to determine which was best suited to this type of prediction. The models were chosen to represent different categories of prediction techniques commonly used: Bayesian density estimation, polynomial curve fitting and neural networks. The specific structures and parameters of each model were chosen to best accommodate our data set and computational constraints. Our results strongly suggest that among the models we tested, the dynamic neural network was the most effective predictor of EMG activity, both within and across subjects.

4.1. Comparison to previous models

The results of our two-dimensional, across-subject tests are directly comparable to those reported by Anderson and

Fuglevand (2008). The predictions generated by their maximum likelihood based model accounted for, on average, 24% of the variance ($r^2 = 0.24$) in the recorded signal. Using the neural network model, here we were able to achieve an overall mean r^2 value of 0.28. This represents a 17% increase in overall prediction accuracy. In addition, we were able to address some of the limitations of the Anderson and Fuglevand model. For example, that model assumed independence between all of the kinematic parameters. This assumption was eliminated by dimensionality reduction in the models tested here. The neural network model was also expanded to deal with movements in three dimensions. A high level of prediction accuracy was maintained (average $r^2 = 0.40$) in the three-dimensional tests; the predictability of some muscles even increased with the introduction of more degrees of freedom. This demonstrates the general applicability of the model to predict muscle activity during complex, unconstrained movements of the upper limb.

4.2. Probability versus determinism

The three different types of models we tested were similar in that they used a large set of training data to determine the most likely level of EMG activity given the kinematic state of the hand. The advantage conferred by the neural network derives from basis functions that are adapted to the particular form of training data—which is a feature of all neural networks—and also from the high level of complexity incorporated into this particular network architecture (many neurons in multiple layers). However, all of the models performed reasonably well. This finding is particularly striking when compared to the performance of deterministic models. These models use inverse dynamics in an attempt to predict muscle torques or muscle activity based on kinematics and physical characteristics of a limb. Such deterministic approaches tend to be complex, typically including a large number of input parameters corresponding to the physical states of the arm and physiological properties of the muscles. For example, Blana *et al* (2008) developed a three-dimensional musculoskeletal model of the upper limb that included 6 bones, 5 joints and 29 muscles. Several elements were used to represent each muscle. Parameters included the positions of joint centres, inertial parameters of the body segments, physiological cross-sectional area of the muscles and pennation angle of every muscle element. This impressive model generated EMG predictions based on limb kinematics with an average r^2 value of 0.21, which is less than what we obtained here using relatively simple probabilistic methods.

Probabilistic models, however, work as 'black boxes' in that they do not provide information about the physical mechanisms responsible for EMG production. Indeed, one important advantage of deterministic models is that they readily enable predictions of motor function associated with, for example, changes in tendon insertion location as might occur with tendon transfer surgery or the outcome associated with stimulating a subset of muscles in a paralyzed limb (Blana *et al* 2008). However, for some FES applications, it may be more important to be able to predict activity patterns efficiently and with high fidelity. Probability-based methods, therefore, may be particularly well suited for these types of applications.

4.3. Limitations

While the neural network model presented here represents an improvement upon the Anderson and Fuglevand model (2008), the model is still limited in its application to many movements. For example, the model does not predict the activity of muscles controlling the digits due to the practical difficulty involved in recording many additional muscles and kinematic parameters. Theoretically, however, there is no reason why the model could not be expanded to include finger movements when such data become available. Additionally, the model does not presently predict changes in muscle activity arising from interactions with objects or external loading, but it should be possible to incorporate information about contact forces into the model. Finally, the model does not account for muscle fatigue. This is a somewhat more difficult problem to address since including information about fatigue would require knowledge about the physiological states of the muscles. Therefore, a more complex network architecture ultimately may be necessary for real-world implementations. Nevertheless, probabilistic approaches show promise for predicting patterns of muscle activity needed to produce complex movements.

Another limitation of the present study was that the movements tested were relatively slow. Subjects were instructed to move at a comfortable speed, and most adopted a moderate pace of movement (see Anderson and Fuglevand (2008)). Previous studies have shown that EMG activity in the arm during slow movements primarily reflects a postural component counteracting the effect of gravity (e.g. Flanders and Soechting (1990), Flanders and Herrmann (1992), Flanders *et al* (1996)). Consequently, the first principal component was dominated by the horizontal position of the hand (figure 6). Little weighting was given to coefficients associated with higher-order kinematic parameters (i.e. velocity and acceleration) suggesting these parameters were not critical for the prediction of EMG signals in the movements tested here. It seems likely that had we tested movements of a more rapid or ballistic nature, higher-order kinematic parameters would have played a more important role in predicting EMG.

Related to practical implementation of the approach outlined here to control an FES-based neuroprosthesis, the pre-processing of the kinematic inputs, including filtering, scaling, differentiation and principal component decomposition, represent non-negligible computational time. This is especially true when the program is run in a high-level application as it currently is. However, because sampling rates are relatively low (30 Hz or less per channel), there may be sufficient time to carry out such pre-processing operations without introducing significant delays. Furthermore, in a clinical application, the flexibility of a software implementation might not be necessary, and some of the delay could be recovered in hardware. Thus, we do not believe that pre-processing presents a significant barrier to real-world applications.

4.4. Application to neuroprosthetics

The long-term objective of this study is to develop a flexible means to control muscle stimulation in an FES-based neuroprosthetic. We envision a three-component system in which (1) the user's intended movement is identified from recordings of activity in the cerebral cortex, (2) such intended movement is translated into a corresponding pattern of muscle activities, and (3) the predicted patterns of muscle activity are realized as a movement of the limb by electrical stimulation of the muscles. Some experimental evidence is available to support, in concept, each of these components. For example, related to the first component, it is known that during actual or imagined movements, the collective activity of populations of neurons in motor regions of the cerebral cortex appears to provide a moment-by-moment representation of the planned trajectory of the limb (Georgopoulos *et al* 1989, Schwartz 1993, Moran and Schwartz 1999, Schwartz and Moran 1999). Similar information has also been shown to be derived from local field potentials (Mehring *et al* 2003, Rickert *et al* 2005, Scherberger *et al* 2005), electrocortigrams (Leuthardt *et al* 2004, Pistohl *et al* 2008) and even from surface EEG signals (Wolpaw and McFarland 2004, Waldert *et al* 2008). Furthermore, this information can be used to control external devices and to interact in real time with the environment (Chapin *et al* 1999, Wessberg *et al* 2000, Serruya *et al* 2002, Musallam *et al* 2004, Velliste *et al* 2008).

Related to the second component, we have shown here that given the desired trajectory of the hand, the time-varying activity patterns in a large number of muscles controlling the upper limb can be predicted. It remains to be seen how effectively these predicted EMG patterns can then be transformed into the desired hand trajectory evoked through electrical stimulation (i.e. the third component). Small prediction errors in each of the individual muscles could add up to significant deviations in the overall evoked movement. Even if the EMG could be perfectly predicted for each muscle, the evoked movements could vary widely across subjects, especially in subjects having different biomechanical properties of the limb. This might be particularly the case for individuals with spinal cord injuries who present with significant muscle atrophy. Additional errors will also be introduced in the transformation of EMG activity into a comparable muscle 'active state' through electrical stimulation. Seifert and Fuglevand (2002), however, were able to evoke a set of desired finger movements using a simple transfer function that converted predicted EMG signals into frequency-modulated patterns of stimulus pulses in several subjects. Furthermore, Hoshimiya *et al* (1989) showed that complicated, coordinated movements of the arm could be evoked in spinal cord injured patients using amplitude-modulated stimulus patterns derived from averaged EMG patterns recorded in healthy subjects. Thus, with respect to the third component, it is possible, at least in some cases, to convert predicted patterns of muscle activity into trains of stimulus pulses needed to evoke desired movements. We are currently exploring ways to optimize this transfer function in order to re-enact the active state of muscle as faithfully as possible represented by EMG signals using electrical stimulation.

All three components of the device that we envision are, therefore, established to some degree. The significant challenge that remains is to link these three components together into a unified system that re-establishes functional communication between the brain and muscles to restore voluntary movements in paralyzed individuals.

Acknowledgments

National Institutes of Health grant NS 061146 supported this work. We thank Dr Chad Anderson for his help with the data collection and advice on analysis.

References

Anderson C V and Fuglevand A J 2008 Probability-based prediction of activity in multiple arm muscles: implications for functional electrical stimulation *J. Neurophysiol.* **100** 482–94

Au A T C and Kirsch R F 2000 EMG-based prediction of shoulder and elbow kinematics in able-bodied and spinal cord injured individuals *IEEE Trans. Rehabil. Eng.* **8** 471–80

Blana D, Hincapie J G, Chadwick E K and Kirsch R F 2008 A musculoskeletal model of the upper extremity for use in the development of neuroprosthetic systems *J. Biomech.* **41** 1714–21

Chapin J K, Moxon K A, Markowitz R S and Nicolelis M A L 1999 Real-time control of a robot arm using simultaneously recorded neurons in the motor cortex *Nat. Neurosci.* **2** 664–70

Cheron G, Draye J P, Bourgeious M and Libert G 1996 A dynamic neural network identification of electromyography and arm trajectory relationship during complex movements *IEEE Trans. Biomed. Eng.* **43** 552–8

Flanders M and Herrmann U 1992 Two components of muscle activation: scaling with speed of arm movement *J. Neurophysiol.* **67** 931–43

Flanders M, Pelligrini J J and Geisler S D 1996 Basic features of phasic activation for reaching in vertical planes *Exp. Brain Res.* **110** 67–79

Flanders M and Soechting J F 1990 Arm muscle activation for static forces in three-dimensional space *J. Neurophysiol.* **64** 1818–37

Georgopoulos A P, Lurito J T, Petrides M, Schwartz A B and Massey J T 1989 Mental rotation of the neuronal population vector *Science* **243** 234–6

Handa Y, Hoshimiya N, Iguchi Y and Oda T 1989 Development of percutaneous intramuscular electrode for multichannel FES system *IEEE Trans. Biomed. Eng.* **36** 705–10

Holm S 1979 A simple sequentially rejective multiple test procedure *Scand. J. Stat. Theory Appl.* **6** 65–70

Hoshimiya N, Naito A, Yajima M and Handa Y 1989 A multichannel FES system for the restoration of motor functions in high spinal cord injury patients: a respiration-controlled system for multijoint upper extremity *IEEE Trans. Biomed. Eng.* **36** 754–60

Hyvarinen A 1999 Survey on independent component analysis *Neural Comput. Surv.* **2** 94–128

Keith M W, Peckham P H, Thrope G B, Buckett J R, Stroh K C and Menger V 1988 Functional neuromuscular stimulation neuroprostheses for the tetraplegic hand *Clin. Orthop. Relat. Res.* **233** 25–33

Kilgore K L, Peckham P H, Thrope G B, Keith M W and Gallaher-Stone K A 1989 Synthesis of hand grasp using functional neuromuscular stimulation *IEEE Trans. Biomed. Eng.* **36** 761–70

Ko W, Liang S and Fung C 1977 Design of radio-frequency powered coils for implant instruments *Med. Biol. Eng. Comput.* **15** 634–40

Koike Y and Kawato M 1995 Estimation of dynamic joint torques and trajectory formation from surface electromyography signals using a neural network model *Biol. Cybern.* **73** 291–300

Leuthardt E C, Schalk G, Wolpaw J R, Ojemann J G and Moran D W 2004 A brain–computer interface using electrocorticographic signals in humans *J. Neural Eng.* **1** 63–71

Manal K and Rose W 2007 A general solution for the time delay introduced by a low-pass Butterworth digital filter: an application to musculoskeletal modeling *J. Biomech.* **40** 678–81

Mehring C, Rickert J, Vaadia E, Cardosa de Oliveira S, Aertsen A and Rotter S 2003 Inference of hand movements from local field potentials in monkey motor cortex *Nat. Neurosci.* **6** 1253–4

Moran D W and Schwartz A B 1999 Motor cortical representation of speed and direction during reaching *J. Neurophysiol.* **82** 2676–92

Musallam S, Corneil B D, Greger B, Scherberger H and Andersen R A 2004 Cognitive control signals for neural prosthetics *Science* **305** 258–62

Peckham P H *et al* 2001 Efficacy of an implanted neuroprosthesis for restoring hand grasp in tetraplegia: a multicenter study *Arch. Phys. Med. Rehabil.* **82** 1380–8

Peckham P H, Kilgore K L, Keith M W, Bryden A M, Bhadra N and Montague M S 2002 An advanced neuroprosthesis for restoration of hand and upper arm control using an implantable controller *J. Hand Surg.* **27** 265–76

Pistohl T, Ball T, Schulze-Bonhage A, Aertsen A and Mehring C 2008 Prediction of arm movement trajectories from ECoG-recordings in humans *J. Neurosci. Methods* **167** 105–14

Rickert J, Cardoso de Oliveira S, Vaadia E, Aertsen A, Rotter S and Mehring C 2005 Encoding of movement direction in different frequency ranges of motor cortical local field potentials *J. Neurosci.* **25** 8815–24

Scherberger H, Jarvis M R and Andersen R A 2005 Cortical local field potential encodes movement intentions in the posterior parietal cortex *Neuron* **46** 347–54

Schieber M H 1995 Muscular production of individuated finger movements: the roles of extrinsic finger muscles *J. Neurosci.* **15** 284–97

Schwartz A B 1993 Motor cortical activity during drawing movements: population representation during sinusoid tracing *J. Neurophys.* **70** 28–36

Schwartz A B and Moran D W 1999 Motor cortical activity during drawing movements: population representation during lemniscate tracing *J. Neurophysiol.* **82** 2705–18

Seifert H M and Fuglevand A J 2002 Restoration of movement using functional electrical stimulation and Bayes' theorem *J. Neurosci.* **22** 9465–74

Serruya M D, Hatsopoulos N G, Paninski L, Fellows M R and Donoghue J P 2002 Instant neural control of a movement signal *Nature* **416** 141–2

Smith B, Peckham P H, Keith M W and Roscoe D D 1987 An externally powered, multichannel, implantable stimulator for versatile control of paralyzed muscle *IEEE Trans. Biomed. Eng.* **34** 499–508

Soechting J F and Flanders M 1997 Evaluating an integrated musculoskeletal model of the human arm *J. Biomech. Eng.* **119** 93–102

Triolo R, Nathan R, Handa Y, Keith M, Betz R R, Carroll S and Kantor C 1996 Challenges to clinical deployment of upper limb neuroprostheses *J. Rehabil. Res. Dev.* **33** 111–22

Valero-Cuevas F J 2000 Predictive modulation of muscle coordination pattern magnitude scales fingertip force magnitude over the voluntary range *J. Neurophysiol.* **83** 1469–79

Velliste M, Perel S, Spalding M C, Whitford A S and Schwartz A B 2008 Cortical control of a prosthetic arm for self-feeding *Nature* **453** 1098–101

Waldert S, Preissl H, Demandt E, Braun C, Birbaumer N, Aertsen A and Mehring C 2008 Hand movement direction decoded from MEG and EEG *J. Neurosci.* **28** 1000–8

Wessberg J, Stambaugh C R, Kralik J D, Beck P D, Laubach M, Chapin J K, Kim J, Biggs S J, Srinivasan M A and Nicolelis M A 2000 Real-time prediction of hand trajectory by ensembles of cortical neurons in primates *Nature* **408** 361–5

Winter D A 2005 *Biomechanics and Motor Control of Human Movement* (New York: Wiley)

Wolpaw J R and McFarland D J 2004 Control of a two-dimensional movement signal by a noninvasive brain–computer interface in humans *Proc. Natl Acad. Sci. USA* **101** 17849–54